

The cataclysmic variable WW Ceti: physical parameters and periodic phenomena[★]

C. Tappert^{1,2}, W.F. Wargau³ **, R.W. Hanuschik², and N. Vogt¹

¹ Astrophysics Group, P.Universidad Católica, Casilla 104, Santiago 22, Chile

² Astronomisches Institut, Ruhr-Universität Bochum, D-44780 Bochum, Germany

³ Dept. of Mathematics and Astronomy, UNISA, P.O. Box 392, 0001 Pretoria, RSA

Received 25 April 1997 / Accepted 30 May 1997

Abstract. We present spectroscopic and photometric data of the cataclysmic variable WW Cet. By comparison of our radial velocity data with earlier published ones we are able to restrict possible orbital periods to the two choices $0.175\,806\,90(25)^d$ and $0.175\,289\,02(35)^d$. We derive an inclination of the system $i = 48(11)^\circ$, which is supported by the fact that the photometric lightcurve shows periodic phenomena folded on the orbital period. These features are identified as a main and an intermediate hump which vary strongly with the brightness level of the system. Our derived periods place them at very unusual phases which do not conform with the normal explanation that the humps are caused by a hot spot which is seen from both front and back. However, our spectroscopy in quiescence indicates that these phasings are real and do not result from an error in the calculation of the ephemerides.

Key words: accretion disks – stars: cataclysmic variables – stars: individual: WW Cet

1. Introduction

A cataclysmic variable (CV) is a binary system which consists of a white dwarf (WD) primary and a late-type secondary. In the general picture, the secondary fills its Roche lobe and thus transfers mass via the Lagrange point L_1 into the region where the gravitational field of the primary dominates. Due to its angular momentum, and in absence of strong magnetic fields, the transferred matter cannot fall directly onto the surface of the WD. By interaction between the particles, an accretion disk is formed around the WD which transports angular momentum to the outer part of the disk and matter to the inner part, i.e. finally

via an inner boundary region onto the surface of the primary. In many cases, the accretion disk never reaches steady state. Its luminosity, released by viscous dissipation within the disk, is strongly variable, with phases of quiescence interrupted by outbursts. Such variability is a common feature of all CVs (for a comprehensive overview on CVs see Warner 1995).

WW Cet was first mentioned as a variable star by Luyten (1962), who already suspected its CV nature, which was later confirmed by Herbig (1962). Paczyński (1963) first published a lightcurve, but could not identify any periodic features. He was also the first to suggest the possibility that the system belongs to the subclass of the Z Cam stars, which are distinguished from other dwarf novae by showing occasionally after an outburst a so-called standstill phase, which can last for weeks or even years. The system has been later indeed included as a Z Cam star in the General Catalogue of Variable Stars (GCVS, Kukarkin et al. 1969).

However, Warner (1987) argued that the long-term behaviour of WW Cet is very untypical of the Z Cam subclass. He instead proposed WW Cet to form a link between dwarf novae and VY Scl nova-like variables. Ringwald et al. (1996), who studied the long-term lightcurve of WW Cet in detail, came to a similar conclusion. This is especially interesting in the context of the hibernation model (Vogt 1982, Shara et al. 1986) which proposes an evolutionary bond between several CV subgroups.

Further long-term photometric data can be found in Bateson & Dodson (1985) and in Bateson & McIntosh (1991). Optical low-resolution spectra have been published e.g. by Williams (1983) (during quiescence) and by Szkody et al. (1990) (near outburst). Klare et al. (1982) and La Dous (1990) present UV spectra, while the X-ray behaviour was studied e.g. by Vrtilik et al. (1994). A finding chart is provided by Downes & Shara (1993).

In this paper, we present new spectroscopic and photometric data on WW Cet. The spectroscopic and photometric measurements are described in Sect. 2, while system parameters are derived from these data in Sect. 3. In Sect. 4 we discuss the

Send offprint requests to: C. Tappert, Bochum address

* based on observations at the South African Observatory in Sutherland, South Africa, and at the European Southern Observatory on La Silla, Chile

** Walter Wargau passed away in 1996 from a long-lasting illness.

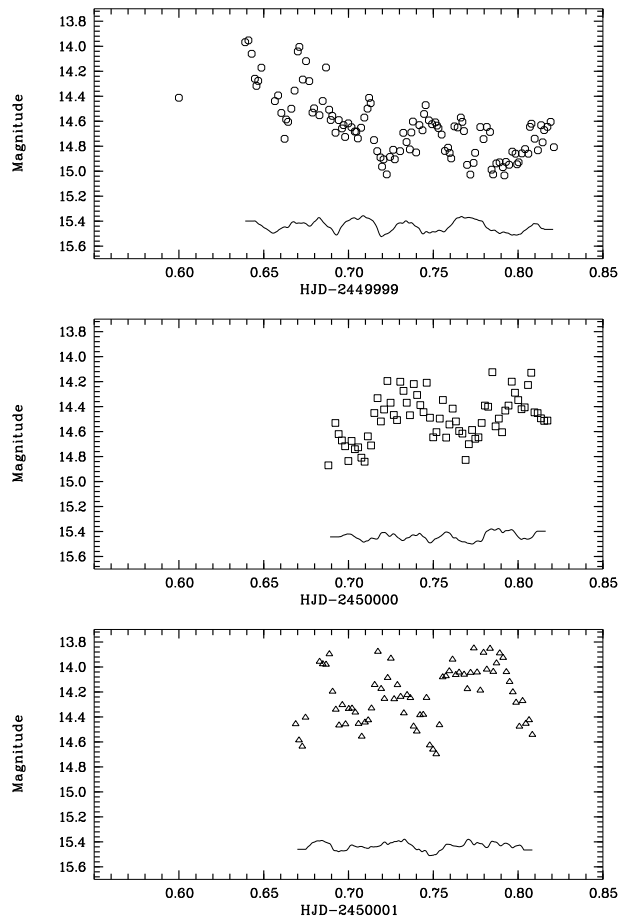


Fig. 1. B photometry for the three nights in 1995: Oct 8 (O), 9 (□), and 10 (△). Magnitudes have been calculated by using calibrated data on comparison stars provided by Misselt (1996). The lines in the lower half of the plots give the B-V behaviour, which was calculated by interpolating the respective photometries. These data have been smoothed and an offset of 15.2 magnitudes has been applied

orbital behaviour of both data sets, and in Sect. 5 we summarize the results.

2. Data

2.1. Time-resolved spectroscopy

WW Ceti was observed with the Image Tube Spectrograph (ITS) combined with the Reticon Photon Counting System (RPCS) mounted on the 1.9 m telescope of the South African Astronomical Observatory in Sutherland, South Africa. In total, 67 measurements have been obtained by one of us (WFW) in 1993 (October 10 and 11) and in 1994 (October 12 and 13). The RPCS collects data in two channels, one containing the object, the other the sky background. These channels have been switched frequently. For our measurements, grating #5 has been used with a dispersion of 50 Å/mm and a total range of 800 Å, centered on H α .

Table 1. Mean photometric values for WW Ceti. The errors give the mean sigma during the night.

Night	V (mag)	B-V (mag)
1995 Oct 08	14.38(25)	0.266(78)
Oct 09	14.26(16)	0.241(73)
Oct 10	13.99(20)	0.238(71)

Observations were done with a 300 μ slit ($\approx 1''.8$), giving a resolution of 1.5 Å. After every 4 exposures, a Ne spectrum was taken for wavelength calibration. Object exposure times were 600–720 s in 1993, and 420 s in 1994. These values were chosen to minimize phase smearing (600 s correspond to 0.04 orbital periods). The S/N for a single spectrum is rather poor, about 7 in 1993 and about 5 in 1994.

The reductions have been done with IRAF¹, using the *noao-onedspec* package. Both channels have been divided by their corresponding flat fields, which were normalized by fitting Chebyshev functions of high order. The background data was then subtracted from the object data. The wavelength calibration of the spectra resulted in a mean *rms* of 0.014 Å, or 0.03 pixel.

Additionally, standard stars have been observed every night, and we therefore also attempted a flux calibration. However, testing our fluxes yielded possible errors as large as 40% due to non-photometric conditions during the observations. We therefore fitted the continuum with low-order Chebyshevs and used these normalized spectra for the further analysis in Sect. 3.1.

2.2. Photometry

We have used the Dutch 0.9 m telescope at the European Southern Observatory, La Silla (Chile) on October 8–10, 1995. We have taken CCD frames in B and V filters with exposure times of 60 and 30 seconds, resp. In the three nights we obtained 10.17 hours of data, but only during the first night we could cover a whole orbital period.

The data of WW Ceti have been reduced with respect to a reference star nearby the object, yielding differential photometry with $\sigma < 0.01$ magnitudes. Comparison with the data on secondary photometric standards published by Misselt (1996) showed that WW Ceti was in quiescence during the observations, with $V \approx 14.2$. Cragg et al. (1995) report the system in outburst on September 28, 1995, but remaining in quiescence during October. Mean magnitudes for the three nights are given in Table 1. All photometric data points are shown in Fig. 1.

¹ IRAF is distributed by the National Optical Astronomy Observatories.

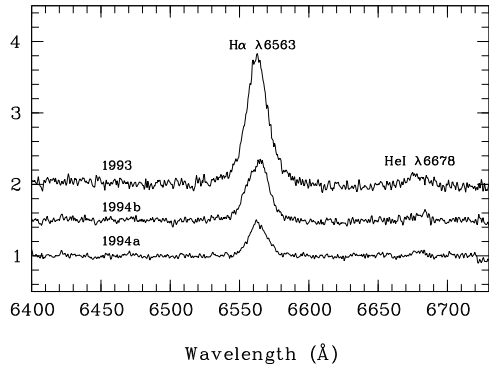


Fig. 2. Averaged normalized ITS spectra of WW Cet. These spectra represent 3 different states, as derived from the continuum flux (see Sect. 3.1): 1993–quiescence, 1994a–outburst, 1994b–decline from outburst. For clarity, offsets of 0.5 and 1.0 units have been applied to separate the spectra

Table 2. Properties of the emission lines in the mean spectra

	1993 quiescence	1994a outburst	1994b decline
H α λ 6563			
equivalent width (\AA)	38(6)	8(1)	17(2)
FWHM (\AA)	20(1)	16(2)	20(1)
FWZI (\AA)	74(6)	41(5)	54(5)
HeI λ 6678			
equivalent width (\AA)	4(3)	1.0(5)	1.4(8)
FWHM (\AA)	24(13)	10(6)	14(8)
FWZI (\AA)	42(14)	30(6)	30(17)

3. Parameters for WW Cet

3.1. The state of WW Cet during the observations

In Fig. 2, we present averaged spectra for each of the three of our observing periods. The typical properties of the lines are summarized in Table 2.

As stated in Sect. 2.1, the flux calibration proved to be very uncertain. However, it is still considered to be good enough to provide some information about the state of WW Cet at the time of our observations. For this reason, we have measured the continuum flux close to the H α line. The first of the data points was taken as reference, while the other values were transformed into magnitudes. The results are plotted in Fig. 3.

These magnitudes show a scatter which amounts within each single data set to $\approx 0^m.8$ in 1993 and $\approx 0^m.5$ in 1994. However, the differences between the 1993 and the 1994 magnitudes are much larger than this, with the 1994 data being much brighter. Furthermore, the second night in 1994 shows WW Cet on a steady decline from the constant level maintained during the first night, almost down to the brightness observed in the 1993 data.

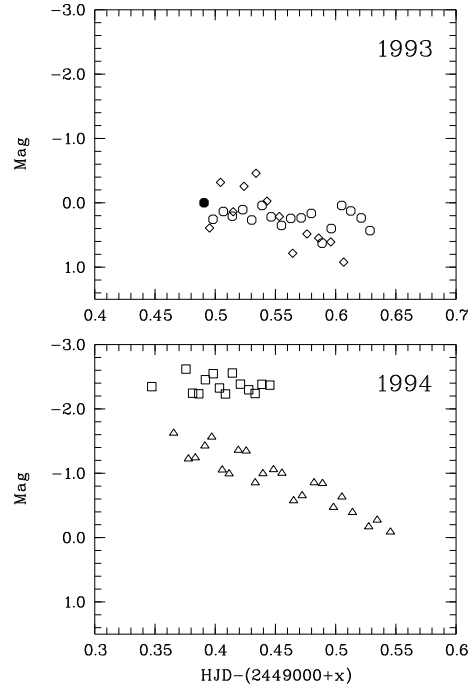


Fig. 3. Continuum flux of WW Cet around the H α line, calculated relatively to the first value of our data set (●). For the different nights, x is 271 (93/10/10, ○), 272 (93/10/11, ◇), 638 (94/10/12, □), and 639 (94/10/13, △)

We conclude that WW Cet was observed in quiescence in October 1993, and in outburst as well as in decline from outburst in October 1994. This is also supported by the observations of the Variable Star Section of the Royal Astronomical Society of New Zealand: our observations in 1993 lie between two registered outburst maxima on JD 2 449 264 and JD 2 449 276 (Jones et al. 1993), and 1 and 2 days after the outburst maximum ($V = 11^m.0$) on JD 2 449 637 in 1994 (Cragg et al. 1994).

3.2. Radial velocities

In order to measure the Doppler shift of the observed line with respect to the rest wavelength of H α , we applied the double Gaussian method as outlined by Shafter (1983). Here, two Gaussians with the same FWHM separated by a wavelength interval d are fitted to the line. By varying the FWHM and d , one is able to measure different parts of the line, i.e. the influence of the line center will increase with increasing FWHM and decreasing d , while narrow Gaussians at wide separation will measure the radial velocities of the line wings.

This method provides an important advantage over a single-Gaussian fit, which does not account for often observed dilution of the disk-born line profile by additional emission sources. However, their influence is irrelevant if we just want to derive the orbital period from the data. At this stage we therefore chose broad Gaussians with FWHM = 40 \AA , measuring those parts of the line with good S/N.

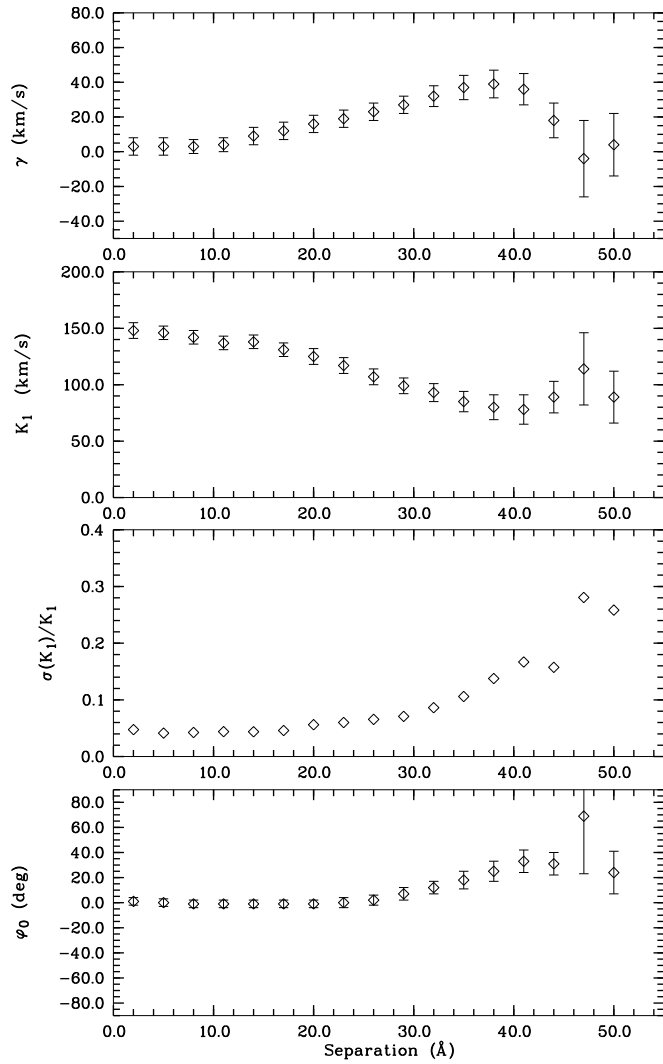


Fig. 4. Diagnostic diagram for the 1993 quiescence radial velocity data measured with a double Gaussian with FWHM = 4 Å

In order to derive the orbital period from these data, we applied both the phase-dispersion minimization method of Stellingwerf (1978) as included in IRAF, and the analysis-of-variance (AOV) algorithm by Schwarzenberg-Czerny (1989) as implemented in the *time-series-analysis* context of MIDAS². While the extracted periods did not differ significantly, the latter method proved more powerful in identifying alias periods.

In earlier radial velocity studies (Kraft & Luyten 1965, Thorstensen & Freed 1985, and Hawkins et al. 1990; these will be referred to hereafter as KL65, TF85, and HJS90, resp.), no unambiguous decision could be made between two periods around 0.150^d and 0.176^d . Such alias problem, however, has been solved recently by Ringwald et al. (1996) (hereafter R96) in favour of the longer period. We therefore refrain from show-

ing the actual periodograms of our study, but only report here our own results, which are

$$P = 0.1767(44)^d \quad \text{and} \quad P = 0.1769(23)^d \quad (1)$$

for the 1993 and 1994 data, respectively. The rather poor precision is probably due to the short overall coverage per orbit (only on 94/10/13 we observed the system for $\gtrsim 1P$).

While the broad Gaussians are sufficient to derive the orbital period, greater care has to be taken when selecting the radial velocities which are used to determine the orbital parameters, i.e. the parameters of the function

$$v_r(\varphi) = \gamma + K_1 \sin(2\pi\varphi), \quad \varphi = (t - T_0) \pmod{P}. \quad (2)$$

As the motion of the WD should be best represented by the variation of the line wings, we used narrow Gaussians with FWHM = 4 Å, which gave the best compromise between high resolution and high S/N for our data. To determine these parameters we used only the quiescence data. The H α line in the outburst data is too narrow for the line wings to be resolved, and the radial velocities of the decline data are probably disturbed by non-orbital changes within the disk (Tappert et al. 1997). The diagnostic diagram for these extracted data is shown in Fig. 4.

In principle one can choose between two possibilities for selecting the separation which corresponds to the correct parameters from this diagram. The first is to look for the minimum value of $\sigma(K_1)/K_1$ as this indicates the best fit to the data. In our case, this separation is 5 Å which is of course much too close to the line center. On the other hand, at some point the line wings will be too much affected by the noise to yield reliable parameters. This point is marked by the last $\sigma(K_1)/K_1$ before the errors increase steeply. Note that this does not *a priori* mean that at this point one has escaped all diluting emission to obtain pure WD motion, but it is probably the best possible approximation which can be extracted from the emission lines.

For our data we have therefore chosen the parameters corresponding to a separation $d = 44$ Å as this provides the last $\sigma(K_1)/K_1 < 0.2$ and the values do not deviate significantly from the ones at $d = 41$ Å. The corresponding parameters are

$$K_1 = 89(14) \text{ km/s} \quad \text{and} \quad \gamma = 18(10) \text{ km/s}. \quad (3)$$

The phase shift between line center and wings is $\Delta\varphi = 30^\circ$, corresponding to ~ 0.08 orbits.

3.3. Towards a more precise orbital period

The publication of four previous radial velocity studies gives us the possibility to determine the orbital period with a much greater precision than before. This can be done by comparing the zero phases of a set of functions from Eq. (2) which are fitted to the single data sets for a sample of periods P within the uncertainty range but with the same T_0 . Here, zero phase refers to the phase φ_0 when the source is in superior conjunction to the observer. In this point the radial-velocity curve fulfills

$$v_r(\varphi_0) = \gamma \quad \text{and} \quad \left. \frac{dv_r}{d\varphi} \right|_{\varphi=\varphi_0} < 0. \quad (4)$$

² MIDAS is provided by the European Southern Observatory, Garching, Germany

Table 3. Results of the frequency search as explained in Sect. 3.3. The upper half of the table gives the frequencies (and their corresponding periods) for the comparison of our 1993 data with TF85, HJS90, and R96. The frequencies of the lower part were determined by including as well our 1994 data and KL65

Frequency (cycles/d)	Period (d)
5.673 381(19)	0.176 261 75(57)
5.681 783(15)	0.176 001 09(46)
5.688 054(12)	0.175 807 07(36)
5.696 461(14)	0.175 547 59(43)
5.704 861(21)	0.175 289 11(65)
5.688 059(8)	0.175 806 90(25)
5.704 864(12)	0.175 289 02(35)

With the combined data of KL65 and our 1994 period spanning a range of 30 years (11018 days), a precision of $\sim 1.3 \times 10^{-7}$ days seems possible if an extrapolation with an accuracy of $0.1P$ is required. However, Fig. 4 shows that the zero point of the radial velocity curve strongly depends on the part of the line it was measured.

The published data of TF85 and R96 were obtained by using two broad Gaussians with FWHM = 40 Å and 45 Å, respectively. Both caught WW Cet in quiescence, and we therefore assume that our 1993 data measured with equally broad Gaussians are quite accurately in phase with these data. On the other hand, HJS90 measured the absorption lines of the secondary which should show exactly opposite phase to the motion of the WD and thus to our 1993 wings data (HJS90 found no significant eccentricity in their radial velocities, and the absorption lines seem thus undisturbed by irradiation effects). We therefore expect that we are allowed to compare these data with an accuracy of $0.1P$.

To choose the frequency range to be searched, we took from all published periods the most accurately determined one from TF85 and allowed a deviation of 5σ . With a precision of 1×10^{-6} cycles/day this gave us a range of 5.667 970 – 5.710 044 cycles/day. We then compared the data sets in pairs by fitting functions of the form in Eq. (2) for each frequency and calculating the zero points according to Eq. (4). The resulting frequencies, i.e. those which give the same phasing (within $0.1P$) for the TF85, R96, and our 1993 broad-Gaussians data on the one hand, and for the HJS90 and our 1993 wings data on the other, are given in Table 3.

Further alias frequencies can be removed by including our 1994 and the KL65 data. However, the phasing of the 1994 data might be somewhat different from the quiescence data (Tappert et al. 1997) and we do not know, to which part of the line the radial velocities of KL65 correspond to. On the other hand, the phases of the line center and the wings in our 1993 data differ for less than 0.1 orbits, and thus we do not expect much bigger differences between any of the data sets.

Therefore, we used for the extended comparison with the 1994 and the KL65 data included an accuracy of $0.2P$ (note that

Table 4. Comparison of our extracted periods with the ones of the single data sets. Not included is the (wrong) period of KL65

Data set	P (d)	$ P - P_1 /\sigma(P)$	$ P - P_2 /\sigma(P)$
1993	0.1767(44)	0.20	0.32
1994	0.1769(23)	0.48	0.70
R96	0.176 53(55)	1.31	2.26
HJS90	0.176 50(88)	0.79	1.38
TF85	0.175 78(13)	0.21	3.78

the largest possible difference is $0.5P$). With this we excluded most of the aliases and are left with only 2 possible frequencies (Table 3). Of these, the period $P_1 = 0.175 806 90^d$ seems the more probable one as it lies near the center of the searched range, while $P_2 = 0.175 289 02^d$ is just at the edge of it, and a comparison with the periods for the single data sets in Table 4 shows that P_1 is in all cases closer than P_2 . The respective dates of the superior conjunction of the WD used for the extrapolations below are therefore $T_0(P_1) = \text{HJD } 2\,449\,271.597\,205\,7$, and $T_0(P_2) = \text{HJD } 2\,449\,271.596\,902\,1$.

3.4. System parameters

With the now established period P and the semiamplitudes K_1 and K_2 we can – under certain assumptions – calculate further physical parameters like mass and radius of the components, and the inclination of the system. For these calculations we will use the period P_1 (results obtained for P_2 do not differ significantly).

Warner (1995) gives semi-empirical relations for mass and radius of the secondary,

$$M_2/M_\odot = 3.453 P^{5/4}, \quad R_2/R_\odot = 2.940 P^{13/12} \quad (5)$$

(P is in days) for $0.054^d \leq P \lesssim 0.375^d$. Thus we obtain for WW Cet $M_2 = 0.393(12)M_\odot$ and $R_2 = 0.447(13)R_\odot$. This is in good agreement with the values for a main-sequence star of spectral type M2-3 (cf. HJS90).

The mass of the WD can be obtained from the semiamplitudes,

$$K_1/K_2 = q = M_2/M_1. \quad (6)$$

Thus $q = 0.397(64)$, $M_1 = 1.05(17)M_\odot$, where we used $K_2 = 224(7)$ km/s from fitting the radial velocities of HJS90 with respect to P_1 . The WD's radius is more difficult to determine, as the chemical composition is unknown, and therefore only rough estimates will be possible. Warner (1995) gives, for a non-rotating helium WD with a mass $0.7 < M_1/M_\odot < 1.3$, the approximation

$$R_1/R_\odot = 0.016(1 - M_1/M_{\text{Ch}}), \quad (7)$$

where $M_{\text{Ch}} = 1.44M_\odot$ is the Chandrasekhar mass. This yields $R_1 = 0.0044(19)R_\odot$. However, we estimate this number a factor 1.5 too low when compared to Fig. 1 of Hamada & Salpeter (1961). Van Amerongen et al. (1987) use

$$R_1/R_\odot = 0.007(M_1/M_\odot)^{-0.8} \quad (8)$$

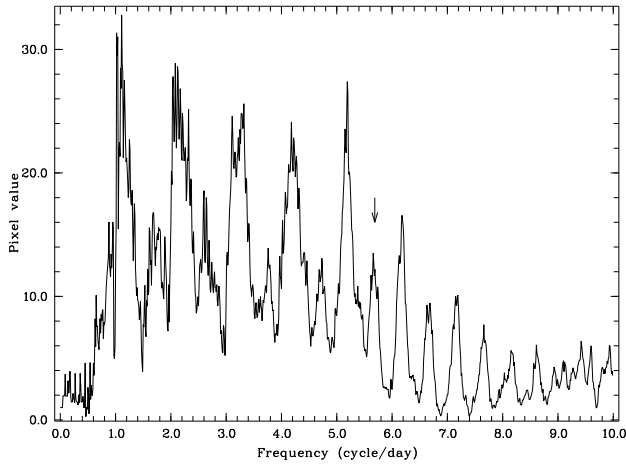


Fig. 5. The resulting periodogram of the AOV analysis of the photometric data. The arrow indicates the orbital period

Table 5. System parameters of WW Cet

$M_2 (M_\odot)$	0.393(12)
$R_2 (R_\odot)$	0.447(13)
$M_1 (M_\odot)$	1.05(17)
$R_1 (R_\odot)$	0.0067(11)
$i (^\circ)$	48(11)

yielding $R_1 = 0.0067(11)R_\odot$ which seems a more reasonable result.

Finally, we can calculate the inclination i of the system. For a Roche-lobe filling secondary,

$$\frac{M_2 \sin^3 i}{(1 + q^{-1})^2} = \frac{K_1^3 P}{2\pi G} \quad (9)$$

which leads to $i = 48(11)^\circ$.

All derived parameters of WW Cet are summarized in Table 5.

4. Orbital variations

The lightcurves are obviously disturbed by strong flickering with amplitudes up to 0.7 mag, consistent with the values given by Bruch (1992). However, they also show variations on timescales much longer than usually conceded to flickering. To search for periodicities, we therefore applied the AOV algorithm to the normalized photometric data (normalization has been performed by subtracting mean values from the individual lightcurves).

The resulting periodogram is shown in Fig. 5. It shows a peak around the orbital period which, however, is by far not the strongest one.

When folded with the orbital period, the photometry reveals two periodic features, a big hump with a width of 0.25 orbital

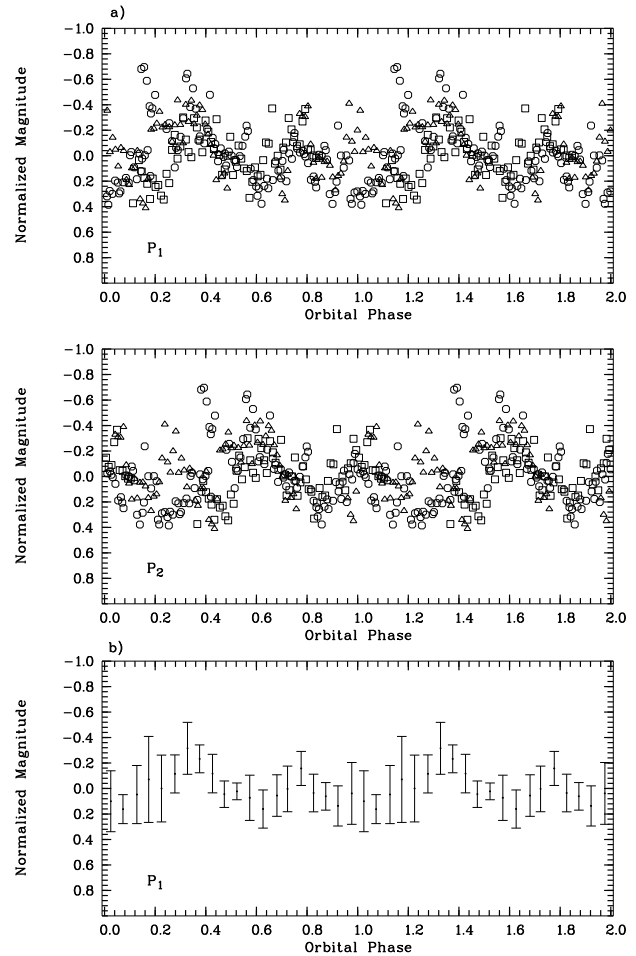


Fig. 6a and b. Lightcurves of WW Cet. **a** The individual lightcurves, derived from the photometric data in Fig. 1. Data are folded on the periods P_1 (top) and P_2 (bottom) taking the zero points T_0 from the spectroscopic data. Magnitudes have been normalized by subtracting the mean value for the respective nights. Two orbits have been plotted for clarity. **b** Mean lightcurve for period P_1 . The mean value of all datapoints within an interval of 0.05 orbital phases has been calculated. Again, two orbits are shown

phases and an 0.15 phases wide small hump (Fig. 6). The distance between the maxima of the big and the small hump, resp., is 0.45 phases, i.e. they are not exactly at opposite phases. When compared to the zero points derived by the spectroscopy, these maxima are at phases 0.33 (big hump) and 0.78 (small hump) for P_1 , and at phases 0.58 and 0.03 for P_2 .

The phenomenon of a main and an intermediate hump is visible in the lightcurves of several CVs and is usually explained with a hot spot visible both from front and back (e.g. Schoembs & Hartmann 1983). These humps are normally more extended than the features in our photometry, but here their structure is severely disturbed by the present strong flickering which is of comparable amplitude. However, both of our possible periods give very unusual phasings as the maximum of the main hump is usually seen just before a photometric eclipse, i.e. around phase 0.9.

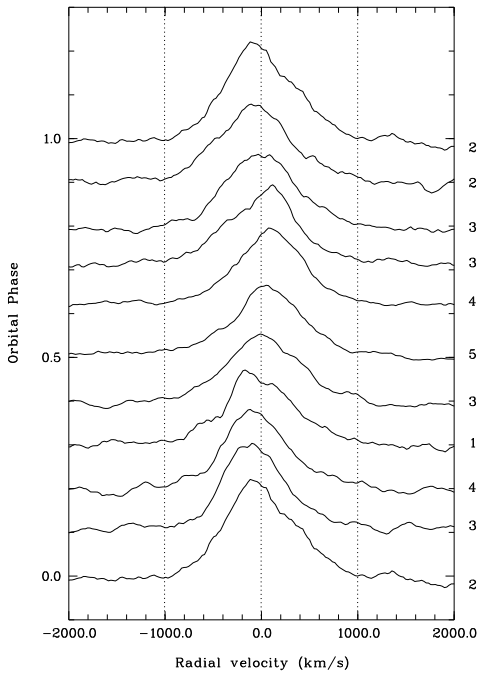


Fig. 7. The 1993 spectroscopic data binned into corresponding phase bins. The data have been corrected for orbital variations with respect to P_1 (there are practically no differences when applying P_2), and they have been smoothed for clarity. The numbers at the right border of the plot give the number of spectra per bin. Phase bin 0.0 is identical to phase bin 1.0.

On the other hand, the spectroscopic data in quiescence give evidence for an unusually located $H\alpha$ emission region (Tappert et al. 1997). In Fig. 7 we show the 1993 data binned into corresponding phase bins. An S-wave with zero points around phases 0.4 and 0.8 is clearly visible. Applying a function of the type in Eq. (2) to the maxima of the spectra yields $\gamma = -41(8)$ km/s, $K_1 = 113(11)$ km/s, and $\varphi_0 = -48(6)^\circ$, i.e. phases 0.13 (superior conjunction) and 0.63 (inferior conjunction). The phases of the maxima of the radial-velocity curve – which correspond to maximum visibility of the source and therefore to possible maxima in the lightcurve – are thus 0.38 and 0.88. Although not being identical, this points in the direction of the phases of the humps with respect to P_1 . This might also be another indication that this is the more probable period.

We also compared the phases of the humps with the published photometries of Paczyński (1963) and Hollander et al. (1993, hereafter HKP93). The values of the corresponding HJDs are given in Table 6. However, when comparing them to Figs. 1 and 9 of Paczyński and HKP93, respectively, no clear evidence for similar features around these times can be found. Possible reasons are the following:

- Our ephemerides are wrong. Although we applied great care when determining them, this is a possibility which cannot be excluded. On the other hand, a time-series analysis of the HKP93 data does not show any indications of the orbital

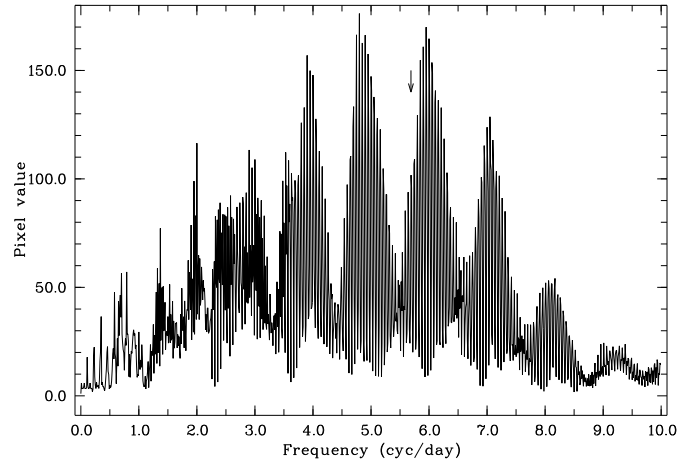


Fig. 8. Time-series analysis of the data of HKP93. The arrow indicates the orbital period

Table 6. Comparison of the phases of the big hump (bh) and the small hump (sh) to the photometries of Paczyński (1963) and Hollander et al. (1993). Given are the HJDs which correspond to the maxima of the humps.

	P_1		P_2	
	φ_{bh}	φ_{sh}	φ_{bh}	φ_{sh}
<u>Paczyński:</u>				
HJD 2 437 967	.799(16)	.702(16)	.835(23)	.738(23)
<u>HKP93:</u>				
HJD 2 447 363	.799(2)	.878(2)	.852(4)	.755(4)
HJD 2 447 382	.786(2)	.865(2)	.783(4)	.862(4)
HJD 2 447 383	.665(2)	.744(2)	.659(4)	.738(4)

period (Fig.8), and it is therefore more probable that the humps are not present in their data.

- The features in our lightcurve are caused by aperiodic variations which just appear to be similar structures at similar phases. This does not sound very convincing either, because our data covers the phases of both humps fully or at least partly for every night.
- The humps are a temporary phenomenon which appeared only recently (i.e. during the last 7 years) or shows up only at certain brightness levels. Paczyński's data shows the system at ~ 13.8 mag, i.e. ~ 0.4 mag brighter than during our observations, while the values given by HKP93 are around 15.0 mag and thus ~ 0.8 mag fainter. Thus Paczyński's data represent quite well the mean quiescence value, while our data lie towards the lower end of the distribution, and HKP93 caught the system at a very rare low brightness (Fig.3 of R96). A with varying brightness disappearing and reappearing intermediate hump has been observed e.g. in VW Hyi (Vogt 1974), and disappearing main humps have been reported for nova-like variables (e.g. Schlegel et al. 1983 for UX UMa in an 0.25 mag brighter state than normal), but to our knowl-

edge there has been no system observed where both humps would disappear.

Convinced of the reality of the humps and their phasing, we are still left with the problem that we find two humps in the lightcurve (with the main one being at superior conjunction) but apparently only one S-wave source. One possibility is that there are two impact regions from the gas stream from the secondary, one at the close and the other at the far side of the disk (seen from the secondary). The $H\alpha$ emission from the first impact region must then be suppressed somehow, possibly hidden by the optically thick stream, as was suggested for RX And by Kaitchuck et al. (1988).

The other possibility is that the stream is spilling over the disk without impacting at the close side (or at least not strong enough to produce $H\alpha$ emission or a photometric hump) producing only one hot spot at the far side of the disk which is then seen both at superior and inferior conjunction. However, for our parameters, the calculations by Lubow (1989) yield an impact site in the inner disk at $0.4 - 0.5 r_d$ (r_d is the disk radius). This corresponds to a much higher velocity than observed (note that the distortion is near the center of the line, i.e. originates from low-velocity material). Another drawback of this scenario is that it fails to explain the phase difference between both humps which departs slightly but significantly from 0.5.

Unfortunately, the S/N of our data is not high enough to really resolve and extract the S-wave contribution. We therefore highly recommend further observations with similar (or better) spectral resolution on bigger telescopes.

5. Summary

We have presented spectroscopic and photometric measurements of the cataclysmic variable WW Ceti. The spectroscopy shows the system in three different states. We have extracted radial velocities and compared them to other authors to derive the orbital period with a precision of 10^{-7} days. We are thus able to constrain the range of possible orbital periods to two choices $P_1 = 0.175\,806\,90(25)^d$ and $P_2 = 0.175\,289\,02(35)^d$, of which the first one seems somewhat more probable. Another time-resolved spectroscopic study in the future might solve this alias problem definitively.

With these periods we have calculated several system parameters for WW Ceti. The derived mass and radius for the secondary are in good agreement with the assumption of a main-sequence star of spectral type M2.5 as already pointed out by HSJ90. The corresponding parameters for the WD suffer from greater uncertainties (due to the large error in K_1 and the uncertain mass-radius relation), but are still in a very reasonable range. Finally, we derived an inclination $i = 48(11)^\circ$ for the system.

The photometric data reveal variations on timescales ~ 1.4 and ~ 0.9 hrs which are periodic with the orbital period and are identified as a main and an intermediate hump. These features as well as the absence of an eclipse support the medium inclination derived by us. Comparison with other photometries showing the system at different brightness levels lets us suspect a temporary

phenomenon which varies with the brightness of the system as has been also observed in other CVs.

When applying the spectroscopic ephemerides, these humps appear at very unusual phases which are not conform with the place which is normally inhabited by the hot spot. On the other hand, the spectroscopic data reveal an enhanced $H\alpha$ emission region in the direction of the phases of the photometric features when they are folded with period P_1 . We therefore believe that this phasing is real.

Future photometric observations of WW Ceti in different brightness states as well as time-resolved spectroscopy with better S/N and time resolution and following Doppler mapping should provide more information on the phenomena described in this paper. Simultaneous observations of absorption and emission lines would allow a direct comparison of their phasings and thus clarify whether the wings of the emission lines really represent the motion of the WD or if additional emission disturbs them as well.

Acknowledgements. CT wishes to thank Thomas Augusteijn and Ronald Mennickent for many ideas and fruitful discussions and for not turning away when being confronted with the behaviour of WW Ceti for the zillionth time. The stay of CT in Chile has been financially supported by the Deutscher Akademischer Austauschdienst (DAAD) under grant D/94/14720. This work has made use of the SIMBAD database which is maintained by the CDS, Strasbourg.

References

- Bateson, F.M. & Dodson, A.W. 1985, Publ. Var. Star. Sec. RASNZ 12, 1
- Bateson, F.M. & McIntosh, R. 1991, Publ. Var. Star. Sec. RASNZ 16, 70
- Bruch, A. 1992, A&A 266, 237
- Cragg, T., Jones, A., Overbeek, D., Taylor, N., Albrecht, W., Murray, A., Turner, D. 1994, Observ. Var. Star Sec. RASNZ M94/10
- Cragg, T., Hull, O., Hovell, S., Jones, A., Overbeek, D., Stubbings, R., Taylor, N. 1995, Observ. Var. Star Sec. RASNZ M95/10
- Downes, R.A. & Shara, M.M. 1993, PASP 105, 127
- Hamada, T. & Salpeter, E.E. 1961, ApJ 134, 683
- Hawkins, N.A., Smith, R.C., Jones, D.H.P. 1990, in: *Accretion-Powered Compact Binaries*, ed.: Mauche, p.113 (HSJ90)
- Herbig, G.H. 1962, Harv. Coll. Obs. Announc. Card 1576
- Hollander, A., Kraakman, H., van Paradijs, J. 1993, A&AS 101, 87 (HKP93)
- Jones, A., Taylor, N., Jones, R., Overbeek, D. 1993, Observ. Var. Star Sec. RASNZ M93/10
- Kaitchuck, R.H., Mansperger, C.S., Hantzios, P.A. 1988, ApJ 330, 305
- Klare, G., Krautter, J., Wolf, B., Stahl, O., Vogt, N., Wargau, W., Rahe, J. 1982, A&A 113, 76
- Kraft, R.P. & Luyten, W.J. 1965, ApJ 142, 1041 (KL65)
- Kukarkin, B.V., Khopolov, P.N., Efremov, Y.U.N., Kukarkina, N.P., Kurochkin, N.E., Medvedeva, G.I., Perova, N.B., Fedorovich, V.P., Frolov, M.S. 1969, *General Catalogue of Variable Stars*, 3rd edition
- La Dous, C. 1990, Space Sci. Rev. 52, 203
- Lubow, S.H. 1989, ApJ 340, 1064
- Luyten, W.J. 1962, Harv. Coll. Obs. Announc. Card 1574
- Misselt, K.A. 1996, PASP 108, 146
- Paczyński, B. 1963, PASP 75, 279

- Ringwald, F.A., Thorstensen, J.R., Honeycutt, R.K., Smith, R.C. 1996, AJ 111, 2077 (R96)
- Schlegel, E.M., Honeycutt, R.K., Kaitchuck, R.H. 1983, ApJS 53, 397
- Schoembs, R. & Hartmann, K. 1983, A&A 128, 37
- Schwarzenberg-Czerny, A. 1989, MNRAS 241, 153
- Shafter, A.W. 1983, ApJ 267, 222
- Shara, M.M., Livio, M., Moffat, A.F.J., Orio, M. 1986, ApJ 311, 163
- Stellingwerf, R.F. 1978, ApJ 224, 953
- Szkody, P., Piché, F., Feinswog, L. 1990, ApJS 73, 441
- Tappert, C., Wargau, W., Hanuschik, R.W. 1997, in: *Proceedings of IAU Coll. 163, Accretion Phenomena and Associated Outflows*, in press
- Thorstensen, J.R. & Freed, I.W. 1985, AJ 90, 2082 (TF85)
- van Amerongen, S., Augusteijn, T., van Paradijs, J. 1987, MNRAS 228, 337
- Vogt, N. 1974, A&A 36, 369
- Vogt, N. 1982, Mitt. Astron. Ges. 57, 79
- Vrtilek, S.D., Silber, A., Raymond, J.C., Patterson, J. 1994, ApJ 425, 787
- Warner, B. 1987, MNRAS 227, 23
- Warner, B. 1995, *Cataclysmic Variables*, Cambridge University Press
- Williams, G. 1983, ApJS 53, 523